# Zirconium phosphate organically intercalated/exfoliated with long chain amine

L. C. Mendes · D. F. Silva · L. J. F. Araujo ·
A. S. Lino

**Abstract** Nanolayered zirconium phosphate was synthesized by the direct precipitation reaction method, and it was organically modified with long chain amine (octadecylamine) at different amine:phosphate ratios (0.5:1, 1:1, and 2:1). Both zirconium phosphate and amine were dispersed in a 2:1 ethanol/water solution. Infrared spectroscopy (FT-IR), thermogravimetry (TG/DTG), differential scanning calorimetry, wide-angle X-ray diffraction (WAXD), and scanning electron microscopy (SEM) were used for characterization. The amine:phosphate ratio regulated the amine insertion in the zirconium phosphate lamellae, as observed by infrared bands, thermal curves, and SEM images. Different TG/DTG degradation temperatures evidenced adsorbed and bonded amine molecules in the phosphate lamellae. Calorimetric results indicated several amine melting temperatures suggesting different crystal arrangements in the phosphate galleries. The presence of octadecylamine changed the crystallographic features of the zirconium phosphate as observed in WAXD.

**Keywords** Octadecylamine · Zirconium phosphate · Exfoliation · Delamination

L. C. Mendes (✉) · D. F. Silva · L. J. F. Araujo
Instituto de Macromoléculas Professora Eloisa Mano,
Universidade Federal do Rio de Janeiro, Avenida Horacio
Macedo, 2030-Centro de Tecnologia, Bloco J, Ilha do Fundão,
Rio de Janeiro 21945-970, Brazil
e-mail: lcmendes@ima.ufrj.br

A. S. Lino
Laboratório de Radioisótopos Eduardo Penna Franca-Instituto de
Biofísica Carlos Chagas Filho, Universidade Federal do Rio de
Janeiro, Rio de Janeiro 21941-902, Brazil

## Introduction

In order to change the chemical and physicochemical characteristics of layered materials, they are reacted with organic molecules. The interest in such reactions is associated with the ability to modify the properties of lamellar fillers by changing their electron density. When successful, the material becomes fully intercalated, consisting of regularly alternating organic and inorganic layers. For nanocomposite preparation, when the filler's galleries are sufficiently delaminated, there is a decrease in interfacial energy between the polymer and inorganic filler. Filler dispersibility has a strong effect on the material's thermal, barrier, and mechanical properties, among others [1–3]. Systems of phyllosilicates/organic molecules have been studied for at least 25 years [4]. Synthetic lamellar phosphates have only recently been gaining importance as alternatives to natural clays, although they have been known since at least the late ninetieth century. The pioneer was alpha-monohydrogen zirconium phosphate, $\alpha$-Zr (HPO$_4$)·2H$_2$O, also called $\alpha$-ZrP [5–7]. This material has acid groups on the inner surface of the layers, which allow direct intercalation of a variety of substances, particularly basic compounds such as alkylamines [8]. High aspect ratio, high cation exchange capacity (*CEC*), and expansion of the lamellae with ion exchange are some features shared by lamellar phosphates and clays [9, 10]. The degree of saturation governs the arrangement of the molecules inside the phosphate galleries. According to Sun et al. [11], a bilayer structure is formed when the amine saturates the lamellar spacing of zirconium phosphate. Above the saturation limit, the amine molecules are oriented according to a variable angle [11–13]. Maximum increase in the interlayer spacing—1.5 nm for ethylamine; 1.7 nm for propylamine and 5 nm for octadecylamine—with intercalation

ratios above 60 % was reported by Dal Pont and coworkers [14]. Espina et al. [15] studied the effect of exposure to alkylamine vapors during 60 days on the intercalation of titanium phosphate. The largest interlayer spacing was obtained for nonylamine, which increased the basal spacing from 1.01 to 2.99 nm. Zirconium phosphate was submitted to expansion with commercial polyetheramine (Jeffamine) Jeffamine at an amine/ZrP molar ratio of 0.75:1 [16]. The authors detected interlamellar expansion of 0.76–3.8 nm. When an amine/ZrP molar ratio of 1:1 at 80 °C was used, the basal spacing changed from 0.76 to 5 nm [17].

The aim of this study was to synthesize α-ZrP lamellar at nanometric scale and to systematically investigate its intercalation with long chain amine (octadecylamine). The platelet/surfactant interactions and the organization of the surfactant in the interlayer space were studied as a function of three amine:ZrP molar ratios (0.5:1, 1:1, and 2:1). The influence of the octadecylamine on the structural, thermal, crystallographic, and morphologic characteristics of the zirconium phosphate was also investigated.

## Experimental

### Materials

Phosphoric acid ($H_3PO_4$), zirconium (IV) oxide chloride 8-hydrate ($ZrOCl_2 \cdot 8H_2O$), and ethanol were supplied by Vetec Ltda. Octadecylamine was purchased from Sigma–Aldrich Ltda.

### Synthesis of layered zirconium phosphate

Layered zirconium phosphate (ZrP) was prepared by the direct precipitation reaction method [18]. A mixture of phosphoric acid ($H_3PO_4$) and zirconium (IV) oxide chloride 8-hydrate ($ZrOCl_2 \cdot 8H_2O$) at [P/Zr] ratio of 18 was maintained under reflux for 24 h [19]. The precipitated crystals were separated by centrifugation, washed with distilled water to pH 6, frozen at −80 °C for 24 h, and lyophilized during 4 days to remove water.

### Modification of zirconium phosphate

The delamination of zirconium phosphate with octadecylamine followed the experimental procedures mentioned by literature [20–22]. Three amine:ZrP molar ratios were applied: 0.5:1, 1:1, and 2:1. Both zirconium phosphate and amine were dispersed in a 2:1 ethanol/water solution. The dispersions were mixed and remained in contact during 24 h, in a 40 °C system. After that, the resulting solid was washed with ethanol to remove unreacted amine and subsequently dried using a lyophilizer.

### Infrared spectroscopy (FT-IR)

Infrared characterization was performed with a Varian Excalibur spectroscope from KBr disks, with 50 scans, resolution of 2 cm$^{-1}$, with the range of 4,000–400 cm$^{-1}$. The main absorptions were identified.

### Wide-angle X-ray diffraction (WAXD)

Wide-angle X-ray diffraction (WAXD) analysis was performed using a Rigaku Miniflex diffractometer with Cu Kα radiation ($\lambda = 0.15418$ nm). The following experimental conditions were used: 30 kV, 20 mA, $2\theta$ interval from 2.0 to 35°, and resolution of 0.01°. Layer spacing ($d$) was calculated using the Bragg relation ($\lambda = 2d \sin \theta$), considering the lower $2\theta$ reflection related to the $hkl$ (002) plane.

### Scanning electron microscopy (SEM)

Scanning electron microscopy (SEM) was performed with a FEI Quanta 400 microscope. After being covered with silver, the sample was bombarded with an electron beam with voltage of 15 kV, and photographs were taken.

### Thermogravimetry (TG/DTG)

Thermogravimetric analysis was carried out with a TA Q500 thermogravimetric analyzer from 0 to 700 °C, 10 °C min$^{-1}$, under nitrogen. The steps and degradation temperatures ($T_{onset}$ and $T_{max}$) and residue were determined. The quantity of amine molecules bonded or adsorbed on zirconium platelets was estimated.

### Differential scanning calorimetry (DSC)

Differential scanning calorimetry (DSC) was performed using a PerkinElmer DSC-7 calorimeter. Each sample was heated from 0 to 190 °C, at 10 °C min$^{-1}$. The sample was kept at 190 °C for 2 min and then cooled to 0 °C at the same scanning rate. A second heating procedure was then performed to 190 °C, at 10 °C. The octadecylamine crystallization ($T_c$) and melting ($T_m$) temperatures were evaluated.

### Hydrogen low-field nuclear magnetic resonance (LFNMR)

In order to assess the polymer relaxation time, $^1$H low-field nuclear magnetic resonance ($^1$HLFNMR) analysis was carried out in a Maran Ultra 23 low-field NMR device. The relaxation time ($T_1H$) was measured from the samples, in time intervals of 10 s and 20 points, at 27 °C. The result was expressed in terms of domain curves.
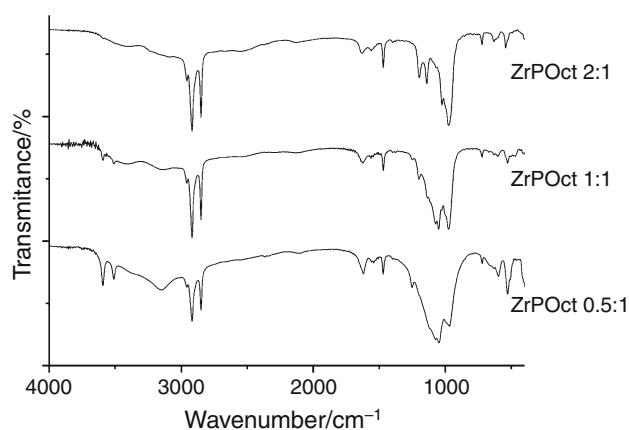
**Fig. 1** FT-IR spectra of phosphate composites

## Results and discussion

### Infrared spectroscopy

The FT-IR spectra of the samples are shown in Fig. 1. The absorptions around 3,593 and 3,511 cm$^{-1}$ associated with the hydrogen bonds of P–OH and H–O–H groups [23] were suppressed in the sample with the highest amine:phosphate ratio. The water molecules were replaced by amine, resulting in the salt PO$^{-+}$H$_3$N(CH$_2$)$_{17}$CH$_3$. The absorption of the P–O bond at 1,050 cm$^{-1}$ did not change for any amine:phosphate ratio. The band at 1,073 cm$^{-1}$ disappeared in the sample where the highest content was applied. The absorption at 1,251 cm$^{-1}$ disappeared, while the band at 967 cm$^{-1}$ was shifted to higher wavenumber as the amine content increased. New bands at 1,198 and 1,140 cm$^{-1}$ were detected due to the increase of amine content. The $^+$H$_3$N group absorptions (1,562 and 1,542 cm$^{-1}$, asymmetric and symmetric angular deformation, respectively) were observed in all modified samples. Octadecylamine absorption bands—2,957, 2,918, 2,850, 1,470, and 720 cm$^{-1}$—were registered. These changes might affect the phosphate crystalline arrangement. There is evidence of intercalation of ZrP layers due to the enlargement and shift of absorption peaks in the region of P–O and P–OH bonds. The interactions formed between different amines and alpha-ZrP on its platelet surface during the intercalation process was observed by Dal Pont et al. [14]. The author remarked that the band shifts are more pronounced, the higher the intercalation degree is.

### X-ray analysis

The WAXD diffractograms of the samples are shown in Figure 2. The WAXD pattern of zirconium phosphate (ZrP) showed the characteristic reflection angles (12.36°

(hkl 002), 20.48°, and 25.61°) and interlayer spacing equal to 0.716 nm, similar to the findings of Brandão et al. [8] and Halim et al. [24]. The diffractogram of the sample with 0.5:1 amine:phosphate ratio presented the original reflection angles of ZrP shifted to 12.25°, 20.25° and 25.54°, and a new crystalline plane appeared at 22.56°, related to the amine diffraction angle. Alberti et al. [25] mentioned that the intercalation of octadecylamine in the gamma-ZrP galleries increased the lamellar spacing from 1.22 to 3.48 nm. The sample with 1:1 amine:phosphate ratio did not show a ZrP diffraction angle at 12.36°. The other peaks decreased in intensity. The amine diffraction peak remained and shifted to a higher angle (23.46°). At the highest amine:phosphate ratio, the sample did not show the crystalline hkl (002) plane. A series of reflection angles between 2 and 10° appeared. These angles are related to the different amine arrangements inside of ZrP galleries. The results indicate that the amine intercalation was successful. Also, a high degree of exfoliation was achieved for the samples obtained from 1:1 and 2:1 amine:phosphate ratios. Thus, the presence of octadecylamine changed the crystallographic features of the alpha-ZrP.

### SEM

The SEM images of alpha-ZrP showed the presence of agglomerated rectangular platelets (Fig. 3). For all amine:phosphate ratios, the platelets were separated due to the insertion of octadecylamine, as depicted in Fig. 4 (1:1 amine:phosphate ratio). The rectangular shape remained even with amine addition. This indicated that the amine molecules are intercalated in both internal surfaces of zirconium phosphate galleries. Considering the SEM images, the length and width of the zirconium phosphate platelets, before and after treatment, were measured (Table 1).The length and width of the zirconium phosphate platelets were very similar. Sun et al. [11] also produced zirconium phosphate using 12 M phosphoric acid at 200 °C, under reflux for 24 h. Lamellae with length between 1,000 and 1,200 nm were obtained, probably due to the effect of the high reaction temperature. Auerbach et al. [4] produced ZrP platelets with width in the range of 600 nm. The SEM result is in agreement with the WAXD analysis.
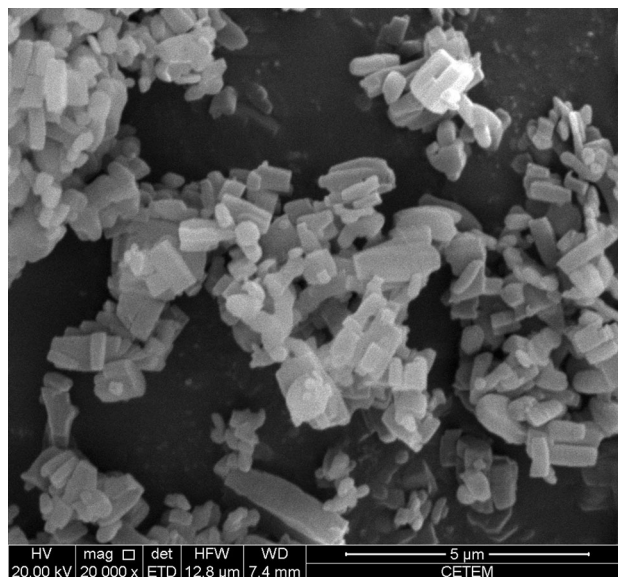
### Thermogravimetry

Thermogravimetric curves and their derivatives are shown in Figs. 5 and 6. Table 2 shows the thermal properties of the precursors and the modified alpha-ZrP at different amine:phosphate ratios. Based on the TG curves, the experimental amine:phosphate ratio was calculated, as well as the chemical formula of each modified phosphate, as reported in Table 2. The neat alpha-ZrP TG curve showed

**Fig. 2** XRD diffractograms for zirconium phosphate and their composites
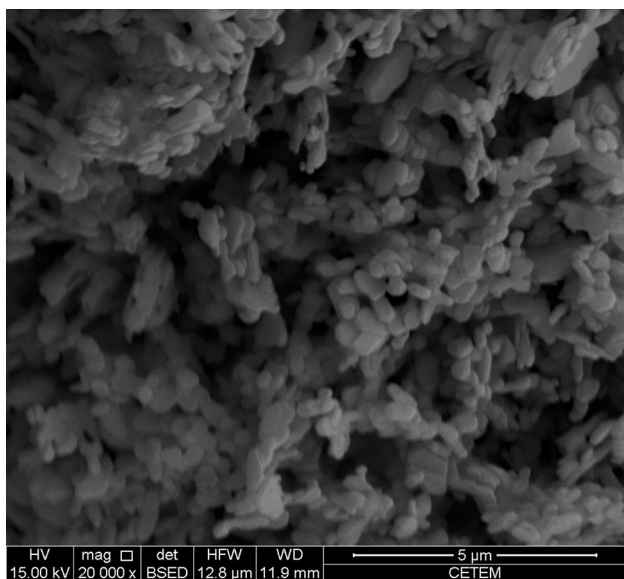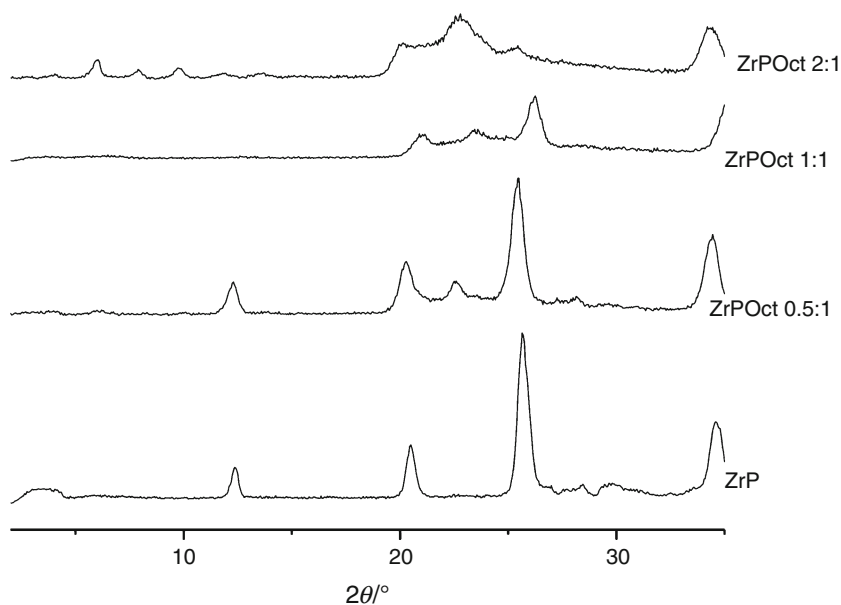


**Fig. 3** SEM micrography of ZrP sample with magnification of ×20,000



**Fig. 4** SEM micrography of ZrPOct 1:1 sample with magnification of ×20,000

two steps of degradation, and dTG presented two derivative peaks. The first was between 100 and 200 °C (maximum at 150 °C), and the second was located between 525 and 625 °C (maximum at 575 °C). They were associated with the release of adsorbed water and the chemical transformation of phosphate to pyrophosphate, as also reported by authors [8, 20]. Octadecylamine degraded in one step, and its dTG curve presented a peak between 125 and 150 °C and a maximum assigned at 225 °C. Three degradation steps were found for the modified phosphate from 0.5:1 amine:phosphate ratio. The derivative peaks were located between 200–275 °C (maximum at 250 °C), 275–375 °C

**Table 1** Length and width values of zirconium phosphate composites platelets measured by SEM

| Samples | Length/nm | Width/nm |
|---|---|---|
| ZrP | 260–740 | 210–480 |
| ZrP:Oct 0.5:1 | 400–990 | 270–450 |
| ZrP:Oct 1:1 | 170–850 | 170–510 |
| ZrP:Oct 2:1 | 160–880 | 190–570 |

(maximum at 350 °C), and 375–425 °C (as shoulder); the last one detected between 525–625 °C, indicating the change of phosphate into pyrophosphate. The first and
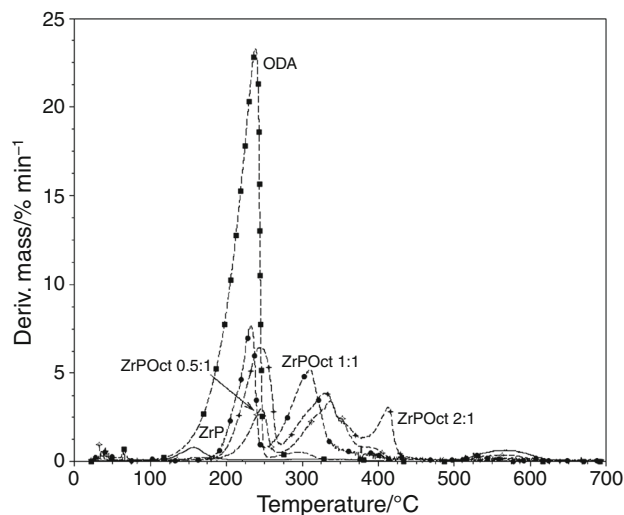
**Fig. 5** TG curves of the precursors and modified phosphate
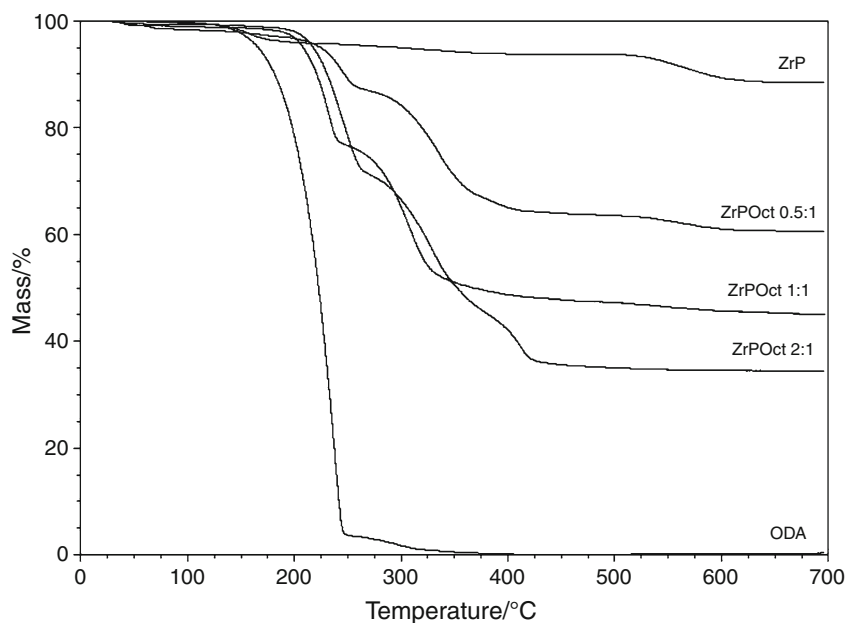
intermediate stages were attributed to the adsorbed and bonded amine in the phosphate galleries, respectively. Some authors [26, 27] have reported that the release of amine at different temperatures is associated with the interaction between P–OH (Brønsted acid) and amine (Brønsted base) groups. The modified phosphate using equimolar ratio of reagents showed two degradation steps. The two dTG peaks were related to the adsorbed and bonded amine, respectively. No phosphate chemical transformation was observed. With excess of amine, the modified phosphate showed three stages of mass loss. The DTG peaks occurred in different temperature ranges. The first appeared at 300–275 °C (release of adsorbed amine). The two other peaks represented amine effectively bonded to the phosphate platelets with different chain arrangements. Also, no transformation of phosphate to pyrophosphate was detected. The degree of insertion of the octadecylamine inside of the phosphate galleries was calculated. The experimental amount of amine on the phosphate surface was similar to the theoretical value. The proposed chemical formula of each modified phosphate is shown in Table 2. The results showed an increase of amine degradation temperature: thermal stability increased by at least 200 °C. According to Figure 7, the highest percentage of amine bonded to phosphate platelets was achieved with a ratio of 0.5:1. The percentage of adsorbed and bonded amine in the phosphate galleries was quasi-similar at higher amine concentrations.

## Calorimetry

The calorimetric curves of the materials—three heating cycles and one cooling cycle—are shown in Figs. 8–11. After the



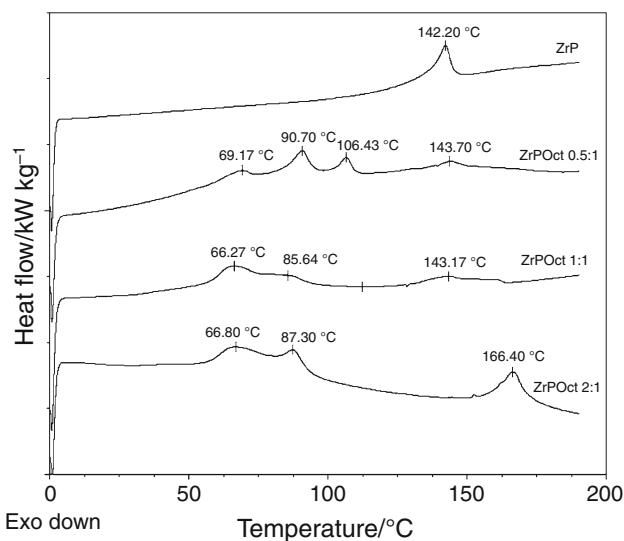**Fig. 6** DTG curves of the precursors and modified phosphate

first heating, alpha-ZrP presented an endothermic peak related to the release of adsorbed water in the galleries. Octadecylamine melting temperature peaks occurred at 54 and 88 °C, the first being sharper and more intense than the second. According to Halim et al. [24], octadecylamine has two endothermic peaks—63 and 89 °C—and the melting at different stages is related to the presence of different crystalline arrangements. For the modified ZrP, no peak was found near 54 °C, indicating the absence of unreacted amine molecules. Nevertheless, a series of endothermic peaks was detected independent of the amine:phosphate ratios. The nature of these peaks was attributed to the different crystalline arrangements. The evaluation of the cooling and second heating cycles was useful. Concerning the cooling cycle, the absence of crystallization peak in the

**Table 2** TG/DTG data for phosphate compounds

| Sample | Formula obtained | Theoretical amine/phosphate ratio | Experimental amine/phosphate ratio | $T_{onset}$/°C | $T_{max}$/°C | Residue/% |
|---|---|---|---|---|---|---|
| ZrP | $Zr(HPO_4)_2 \cdot 0.92\ 2H_2O$ | – | – | 133.91 | 157.27 | 88.4 |
| | | | | | 327.79 | |
| | | | | | 568.17 | |
| ODA | $C_{18}H_{39}N$ | – | – | 202.64 | 237.95 | 0.33 |
| ZrPOct 0,5:1 | $Zr(HPO_4)2 \cdot (C_{18}H_{39}N)_{0.5345} \cdot 0.5789H_2O$ | 0.5 | 0.5445 | 225.25 | 65.16 | 60.56 |
| | | | | | 245.80 | |
| | | | | | 337.31 | |
| | | | | | 566.85 | |
| ZrPOct 1:1 | $Zr(HPO_4)2 \cdot (C_{18}H_{39}N)_{1.0989} \cdot 0.5112H_2O$ | 1 | 1.1268 | 211.43 | 232.61 | 45.06 |
| | | | | | 283.23 | |
| | | | | | 310.88 | |
| ZrPOct 2:1 | $Zr(HPO_4)2 \cdot (C_{18}H_{39}N)_{1.7992} \cdot 0.1359H_2O$ | 2 | 1.9423 | 217.74 | 243.31 | 34.50 |
| | | | | | 331.56 | |
| | | | | | 412.92 | |
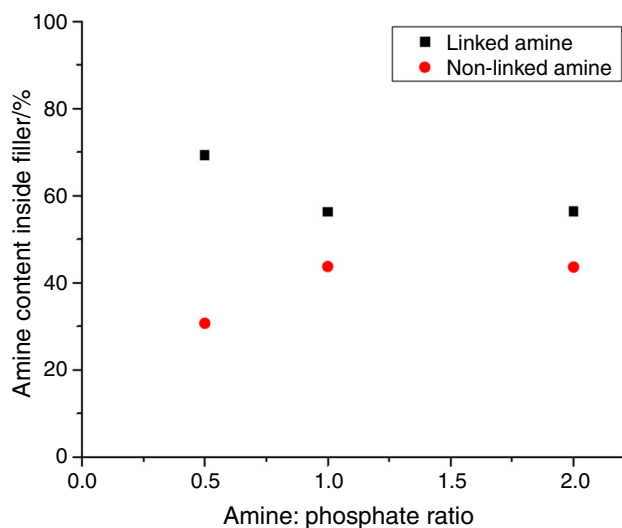


**Fig. 7** Amine content linked and non-linking inside zirconium phosphate galleries with different intercalation ratios
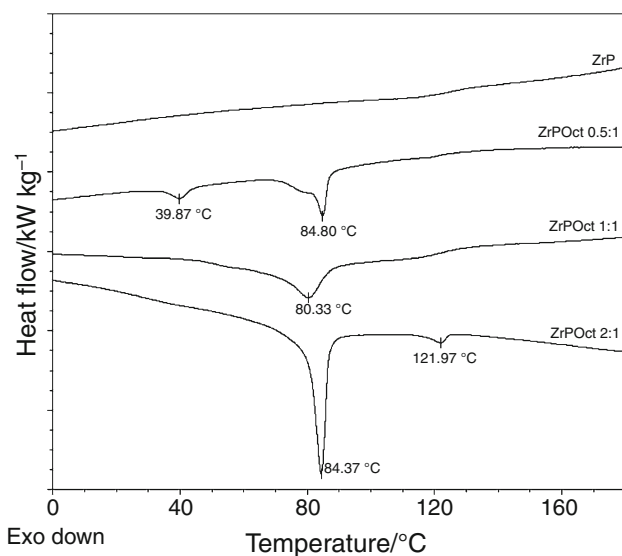


**Fig. 8** First heating for phosphate composites

curve of the alpha-ZrP confirmed the release of water in the first heating cycle. The two crystallization peaks of octadecylamine are in agreement with what was found in the first heating cycle. For the modified alpha-ZrP, it can be inferred that the peaks registered in the first heating cycle at 143, 142, and 166 °C (amine:phosphate ratios of 0.5:1, 1:1, and 2:1, respectively) were associated with the release of water. Although in the cooling cycle, only one crystallization peak appeared for modified alpha-ZrP, and the other peaks detected in the first heating cycle were related to the crystalline melting temperature of the amine. They represent amine molecules randomly organized inside the galleries as adsorbed or bonded molecules on the zirconium phosphate surface. The initial cycles of heating and

cooling destroyed the original crystalline arrangement of the amine on the modified phosphate surface. In the second heating cycle, the curves for modified zirconium phosphate showed melting peaks at different temperatures. This is associated with different crystalline arrangements and interactions of amine on the zirconium phosphate surface, as adsorbed and chemically bonded molecules. The result is in agreement with thermogravimetry and WAXD analyses.
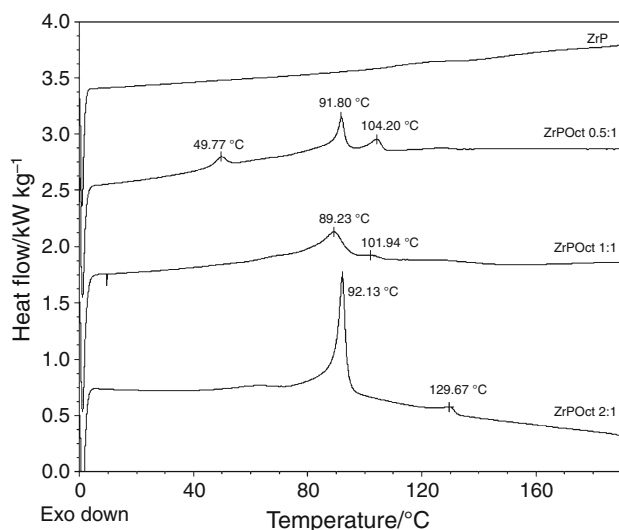
Hydrogen low-field nuclear magnetic resonance

The low-field nuclear magnetic resonance (LFNMR) is a powerful tool for determining molecular relaxation in
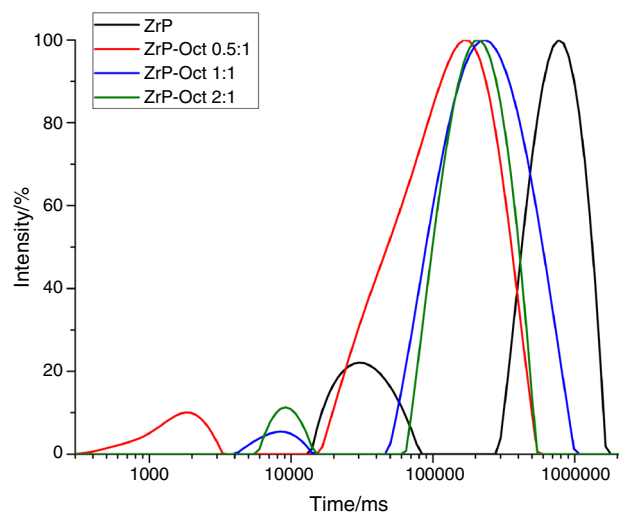
Fig. 9 First cooling for phosphate composites
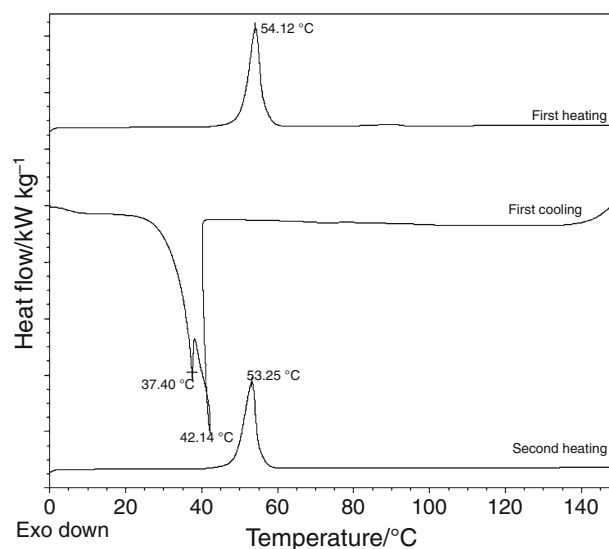


Fig. 11 DSC for octadecylamine



Fig. 10 Second heating for phosphate composites



Fig. 12 Domain curves for ZrP and the ZrP-Octadecylamine fillers

organic/inorganic chemical structures. Brito et al. [28] studied the intercalation of clays in potato starch and showed that the decrease in relaxation times ($T_1H$) is related to exfoliation of the material. Bruno et al. [29] also studied the NMR to investigate exfoliation/dispersion of clays in PHB matrix. In this work, hydrogen low-field NMR was used in order to evaluate the effect of octadecylamine at different ratios on the structural arrangement of ZrP. Figure 12 shows the domain curves of neat ZrP and modified ones. The neat ZrP curve presented a bimodal relaxation peak with different intensities and the values of relaxation times. The first one is located around 10,000–100,000 ms, while the second one is between 300,000 and 2,000,000 ms. We can suppose that the difference is related to the

existence of ZrP structures with different number of platelets. The lowest peak possesses less platelets, and the structure relaxed at low relaxation time. On the contrary, the highest peak represented the relaxation of ZrP structure with large number of platelets, which demand high relaxation time for relaxing. The outline of ZrP domain curves modified with octadecylamine is similar to the precursor, but the relaxation times were shifted to low values (Table 3). The ZrPOct with amine:phosphate ratio of 0.5:1 showed the lowest relaxation time. The peak at highest relaxation time is broad indicating the effectiveness of the octadecylamine inside the filler galleries. The insertion of octadecylamine reduced the packing of the ZrP platelets

**Table 3** $T_1H$ obtained for ZrP and the ZrP-octadecylamine fillers

| Samples | $T_1H$/ms | $T_1H$ domain/% |
|---|---|---|
| ZrP | 30.13 | 27.79 |
| | 767.32 | 72.21 |
| ZrP Oct 0.5:1 | 1.94 | 4.55 |
| | 183.12 | 95.45 |
| ZrP Oct 1:1 | 8.32 | 2.36 |
| | 225.30 | 97.64 |
| ZrP Oct 2:1 | 8.49 | 4.82 |
| | 199.17 | 95.18 |

due to the increase of the amount of hydrogen in the structure. Then, the chain molecular mobility increased, and the value of relaxation time decreased. We can also assume that the broad peak represents the average of the contribution of relaxations of intercalated, pre-exfoliated, and exfoliated structures of modified ZrP. The domain curves of ZrPOct with amine:phosphate ratios of 1:1 and 2:1 were very similar. It can be observed that the curve of ZrPOct 1:1 is broader than ZrPOct 2:1, but narrower than ZrPOct 0.5:1. This can indicate that the arrangement of the octadecylamine molecules is randomic along of the ZrP stacks. Also, the structural homogeneity was reached at high amine:phosphate ratio.

## Conclusions

Nanolamellar α-ZrP was synthesized and modified with octadecylamine with three amine:ZrP molar ratios (0.5:1, 1:1, and 2:1). The platelet/surfactant interactions and the organization of the surfactant in the interlayer space were studied. The modification was successful. The amine:phosphate ratio governed the amine insertion in the zirconium phosphate lamellae. The effect of the amine on the alpha-ZrP interlayer spacing was strong at higher amine:phosphate ratios, as detected by WAXD. Infrared analysis, showing enlargement and shift of phosphate absorption bands, and thermal analysis, indicating melting and release of amine molecules at different temperatures, evidenced that a Brønsted acid–base reaction between P–OH (Brønsted acid) and amine (Brønsted base) groups occurred. Adsorbed and linked amine molecules were observed in the phosphate lamellae. The material has strong potential for use as lamellar filler in polymeric nanocomposites.

## References

1. Burwell DA, Thompson ME. Synthesis of amide-functionalized and ester-functionalized zirconium phosphonates. Chem Mater. 1991;3(4):730–7.
2. Cardoso WD, Gushikem Y. Preparation of lamellar compounds: synthesis of the crystalline zirconium hydrogen phosphate and its intercalation with amines. An experiment for undergraduate students. Quim Nova. 2005;28(4):723–6.
3. Herrera-Alonso M, Abdala AA, McAllister MJ, Aksay IA, Prud'homme RK. Intercalation and stitching of graphite oxide with diaminoalkanes. Langmuir. 2007;23(21):10644–9. doi:10.1021/1a0633839.
4. Auerbach SM, Carrado KA, Dutta PK. Handbook of layered materials. M. Dekker. New York: CR Press, 2004.
5. Mahfuz H, Adnan A, Rangari VK, Hasan MM, Jeelani S, Wright WJ et al. Enhancement of strength and stiffness of Nylon 6 filaments through carbon nanotubes reinforcement. Appl Phys Lett. 2006;88(8). doi:10.1063/1.2179132.
6. Clearfield A, Stynes JA. The preparation of crystalline zirconium phosphate and some observations on its ion exchange behaviour. J Inorg Nucl Chem. 1964;26(1):117–29.
7. Szirtes L, Riess L, Megyeri J, Kuzmann E. Comparative study of layered tetravalent metal phosphates containing various first-row divalent metals. Synthesis, crystalline structure. Cent Eur J Chem. 2007;5(2):516–35. doi:10.2478/s11532-007-0003-2.
8. Brandao LS, Mendes LC, Medeiros ME, Sirelli L, Dias ML. Thermal and mechanical properties of poly(ethylene terephthalate)/lamellar zirconium phosphate nanocomposites. J Appl Polym Sci. 2006;102(4):3868–76. doi:10.1002/app.24096.
9. Nancollas GH, Tilak BVKSRA. Thermodynamics of cation exchange on semi-crystalline zirconium phosphate. J Inorg Nucl Chem. 1969;31(11):3643–53. doi:10.1016/0022-1902(69)80352-0.
10. Ramis LB. Compósitos termoplásticos contendo fosfatos e fosfonatos lamelares de zircônio e Titânio, (Thesis in Polymer Science): Universidade Federal do Rio de Janeiro, Rio de Janeiro RJ, 2007.
11. Sun LY, O'Reilly JY, Kong DY, Su JY, Boo WJ, Sue HJ, et al. The effect of guest molecular architecture and host crystallinity upon the mechanism of the intercalation reaction. J Colloid Interface Sci. 2009;333(2):503–9. doi:10.1016/j.jcis.2009.02.028.
12. Nunes LM, Airoldi C. Lamellar titanium hydrogenphosphate: synthesys, ion-exchange and intercalation. Quim Nova. 2001;24(6):799–807.
13. Vaia RA, Teukolsky RK, Giannelis EP. Interlayer structure and molecular environment of alkylammonium layered silicates. Chem Mater. 1994;6(7):1017–22.
14. Dal Pont K, Gerard JF, Espuche E. Modification of alpha-ZrP nanofillers by amines of different chain length: Consequences on the morphology and mechanical properties of styrene butadiene rubber based nanocomposites. Eur Polym J. 2012;48(1):217–27. doi:10.1016/j.eurpolymj.2011.11.006.
15. Espina A, Menendez F, Jaimez E, Khainakov SA, Trobajo C, Garcia JR, et al. Intercalation of alpha, omega-alkyldiamines into layered A-titanium phosphate from aqueous solutions. Mater Res Bull. 1998;33(5):763–71.
16. Boo WJ, Sun L, Liu J, Moghbelli E, Clearfield A, Sue H-J et al. Effect of nanoplatelet dispersion on mechanical behavior of polymer nanocomposites. J Polym Sci B Polym Phys. 2007;45(12). doi:10.1002/polb.21163.
17. Sue HJ, Gam KT, Bestaoui N, Spurr N, Clearfield A. Epoxy nanocomposites based on the synthetic alpha-zirconium phosphate layer structure. Chem Mater. 2004;16(2). doi:10.1021/cm030441s.

18. Alberti G. Syntheses, crystalline-structure, and ion-exchange properties of insoluble acid salts of tetravalent metals and their salt forms. Acc Chem Res. 1978;11(4):163–70. doi:10.1021/ar50124a007.

19. Clearfield A, Smith GD. Crystallography and structure of.alpha.-zirconium bis(monohydrogen orthophosphate) monohydrate. Inorg Chem. 1969;8(3):431–6. doi:10.1021/ic50073a005.

20. Mendes LC, Silva DF, Lino AS. Linear low-density polyethylene and zirconium phosphate nanocomposites: evidence from thermal, thermo-mechanical, morphological and low-field nuclear magnetic resonance techniques. J Nanosci Nanotechnol. 2012;12(12):8867–73. doi:10.1166/jnn.2012.6718.

21. Perez-Santano A, Trujillano R, Belver C, Gil A, Vicente MA. Effect of the intercalation conditions of a montmorillonite with octadecylamine. J Colloid Interface Sci. 2005;284(1):239–44. doi:10.1016/j.jcis.2004.09.066.

22. Weiss Z, Valaskova M, Kristkova M, Capkova P, Pospisil M. Intercalation and grafting of vermiculite with octadecylamine using low-temperature melting. Clays Clay Miner. 2003;51(5):555–65. doi:10.1346/ccmn.2003.0510509.

23. Diaz A, Mosby B, Mejia AF, Batteas JD, Cheng Z, Clearfield A. Self-assembled monolayers based upon a zirconium phosphate platform. Chem Mat. 2013;55(5):723–728.

24. Halim NA, Ibrahim ZA, Ahmad AB. Intercalation of water and guest molecules within Ca(2+)—montmorillonite. J Therm Anal Calorim. 2010;102(3):983–8. doi:10.1007/s10973-010-0860-3.

25. Alberti G, Marmottini F, Cavalaglio S, Severi D. Intercalation processes of n-alkyl monoamines in gamma-zirconium phosphate. Langmuir. 2000;16(9):4165–70.

26. Clearfield A, Thakur DS. The acidity of zirconium-phosphates in relation to their activity in the dehydration of cyclohexanol. J Catal. 1980;65(1):185–94.

27. Kurokawa H, Ohshima M, Sugiyama K, Miura H. Methanolysis of polyethylene terephthalate (PET) in the presence of aluminium tiisopropoxide catalyst to form dimethyl terephthalate and ethylene glycol. Polym Degrad Stab. 2003;79(3):529–33. doi:10.1016/s0141-3910(02)00370-1.

28. Brito LM, Tavares MIB. Desenvolvimento de nanocompósitos à base de amido de batata. Polímeros. 2013;23(6):771–7.

29. Bruno M, et al. Evaluation of PHB/Clay nanocomposite by spin-lattice relaxation time. Mat Res. 2008;11(4):483–5.